Title
Understanding the Bias Introduced in Quantum Dot Blinking Using Change Point Analysis

Journal
The Journal of Physical Chemistry C, 120(51)

ISSN
1932-7447

Authors
Bae, Youn Jue
Gibson, Natalie A
Ding, Tina X
et al.

Publication Date
2016-12-29

DOI
10.1021/acs.jpcc.6b09780

Peer reviewed

THE JOURNAL OF PHYSICAL CHEMISTRY C

Article

pubs.acs.org/JPCC

Understanding the Bias Introduced in Quantum Dot Blinking Using Change Point Analysis

Youn Jue Bae,[†] Natalie A. Gibson,[†,∥] Tina X. Ding,[†,§,#] A. Paul Alivisatos,[†,§,⊥,#] and Stephen R. Leone*[,†,‡,∥]

[†]Department of Chemistry, [‡]Department of Physics, and [§]Department of Materials Science and Engineering, University of California, Berkeley, Berkeley, California 94720, United States

[∥]Chemical Sciences Division and [⊥]Materials Sciences Division, Lawrence Berkeley National Laboratory, Berkeley, California 94720, United States

[#]Kavli Energy NanoScience Institute, Berkeley, California 94720, United States

Supporting Information

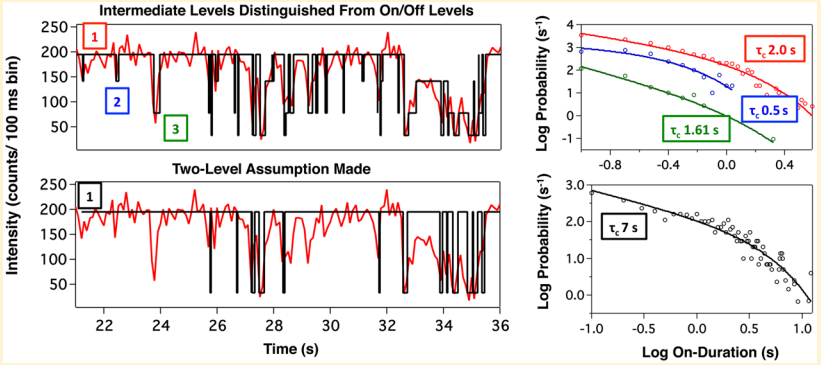

ABSTRACT: The fluorescence intermittency of single CdSe/CdS quantum dots (QDs) with different shell sizes is studied using the conventional bin and threshold method and the statistically more rigorous method, change point analysis (CPA). The on-state truncation time (τ_c) is a critical value used to interpret the dynamics of charge trapping in single QDs; however, changing the bin size and threshold in blink traces significantly modifies τ_c. Herein, we use the CPA method to minimize the bias that binning and thresholding introduces and find that a widely used assumption that there is only one on and one off state is questionable. We observe that 12 out of 17 QDs exhibit more than two intensity levels and find that the τ_c values of individual levels differ from the values obtained when the levels are combined, i.e., when one assumes there is only one on and one off state as in the conventional bin and threshold method. For instance, one QD has τ_c values of 0.5 (0.1) and 2.0 (0.2) s from two different intensity levels, whereas when the levels are combined into only one on state, τ_c is found to be 7 (1) s. The CPA method is found to be more suitable for studying multilevel emission in QDs than the conventional bin and threshold method.

INTRODUCTION

There have been a substantial number of studies regarding the fluctuations of emission intensity, known as fluorescence intermittency or blinking, in single colloidal semiconductor nanocrystals, or quantum dots (QDs), and various models describing the underlying charge carrier trapping kinetics of blinking have been proposed.[1−3] To analyze blinking in QDs, a time series of emission intensities, referred to here as a blink trace, is constructed traditionally by binning the arrival times of emitted photons and setting a threshold to distinguish on and off states. Probability distributions for durations of on states and off states can then be obtained. Studies have shown that the probability distributions ($P(\tau)$) of the on and off time durations follow an exponentially truncated power law, $P(\tau) \propto \tau^{-m} e^{-\tau/(\tau_c \text{ or } \tau_d)}$, where blinking frequency can vary over 6 orders of magnitude in time.[4,5] A truncation time or the time constant corresponding to rapid fall-off from power-law behavior is observed for both on (τ_c) and off (τ_d) probability distributions, and the power-law exponent (m) is typically observed to be less than 2.[6]

Although the bin and threshold analysis is the most commonly used method for evaluating the kinetics of QD blinking, recent papers have raised the point about its unavoidable bias.[7−10] In this method, binning is necessary to reduce Poissonian counting noise and to isolate emission states; however, the choice of bin time introduces an artificial time scale to the measurement, and depending on the bin time, certain information can be lost or favored. For instance, a longer bin time is incapable of detecting fast events whereas a shorter bin time prevents an accurate separation of emission

Received: September 27, 2016
Revised: November 20, 2016
Published: December 7, 2016

DOI: 10.1021/acs.jpcc.6b09780
J. Phys. Chem. C 2016, 120, 29484−29490

states.[7] According to the work of Crouch et al., changing the bin size from 1 to 100 ms was shown to increase the on-state truncation time from 0.6 (0.1) to 1.2 (0.4) s in one sample QD.[8] One approach to address this issue is to directly incorporate photon binning into blinking models,[11,12] but since this approach must be carried out within each individual model, its broad applicability is restricted. Rather than requiring theoretical models to incorporate externally imposed time scales into detailed kinetic schemes, another strategy would be to process photon arrival times via a bin-free, model-free analysis method. Toward this goal, Watkins and Yang developed a quantitative and statistically robust method called change point analysis (CPA).[7]

Unlike binning and thresholding where the probability distributions are derived from averaging the number of photons, CPA accounts for every photon count recorded. In the CPA algorithm, a generalized likelihood ratio test is used to identify intensity change points. The probability that the observed data contain an intensity change point is calculated and compared to the probability that there was no change point. From this, the locations of where the change points occur throughout a blink trace can be found. Along with the position, a confidence region for the position of the change point (the possible range of the position) and confidence level (how certain the location is) are obtained.[7] Lastly, using the Bayesian information criterion, various detected change points are clustered into a finite number of discrete intensity levels. As a result, both the number and location of intensity changes are found, and a blink trace that is free of binning can be reconstructed. Alternative bin-free analyses do exist that are either based on power spectral densities[4,13,14] or autocorrelation functions.[9,15] These methods can be very fast, enabling large sample sizes to be investigated, but typically they cannot be used to independently extract on and off state kinetics. A recent autocorrelation analysis was able to determine both on and off power-law exponents by making use of a few assumptions including that all QDs in a batch of data have identical exponents.[9] Since it is beneficial to investigate the bias associated with binning and thresholding without restricting the kinetics of each QD (power-law exponents, number of intensity levels), CPA is the most suitable bin-free analysis method to employ in the current study.

In this paper, the blinking kinetics of single CdSe/CdS core/shell QDs consisting of two different shell thicknesses were analyzed. Blinking in this material has largely been found to deviate from the characteristic binary behavior often reported for CdSe QDs capped with ZnS shells.[4,16−19] The blinking kinetics were first examined using the bin and threshold method to identify any bias such a method introduces. Subsequently, CPA was carried out and the number of intensity levels determined. We compared the τ_c values of individual levels to the truncation times calculated by assuming the presence of only two levels and found a discrepancy between τ_c values.

METHODS

The CdSe/CdS nanocrystals used in this work were synthesized following an adaptation of a procedure previously detailed by Chen et al.[20] The core size was 3.7 (0.26) nm, and the shell thickness was either 11.9 monolayers (MLs) for the 12 (1.3) nm QDs or 4.3 MLs for the 6.8 (0.3) nm QDs, where 1 ML = 0.35 nm. TEM, absorption and photoluminescence spectra, and quantum yield information for the two samples are summarized in Figure S1. Dilute QD solutions were drop-cast onto fused silica coverslips to achieve dispersed samples with concentrations <0.01 QD/μm^2. The samples were mounted in a modified Olympus IX71 inverted confocal microscope, equipped with piezoelectric $x-y$ (PI 517) and z (home-built from Thorlabs AE0505D16F) stages for alignment and focus.

The second harmonic (400 nm) of the output of a Coherent RegA 9000 amplifier (800 nm, 200 fs, 295 kHz) seeded by a Coherent Mira 900 oscillator was used as the pulsed excitation source. The 400 nm light was transmitted through neutral density filters to achieve a low probability of exciton formation per pulse ($\langle N_{ex} \rangle \approx 0.005$) and focused by a ×100, 1.3 NA oil-immersion objective (Nikon PlanFluor) onto the sample surface. The fluorescence from individual QDs was collected in an epifluorescence scheme, filtered by a dichroic (Semrock Di405) and short-pass and long-pass filters, and focused onto two avalanche photodiodes (MPD PDM-50 series) input to a time-correlated single photon counting (TCSPC) module (PicoQuant PicoHarp300/PHR 800). The overall instrument response was ∼30 ps.

Photon arrival times were recorded for 10 min via TCSPC for all QDs. The 17 QDs analyzed in this study were selected on the basis of displaying the best photon antibunching, meaning the area of the zero time delay peak divided by the mean of the subsequent three peaks was less than 0.1 without a background subtraction (Figure S2). For the bin and threshold analysis, blink traces were produced by choosing bin sizes of 10, 50, and 100 ms. To separate into a series of on and off durations, a threshold was set to be just above the off-state peak by analysis of the intensity histogram.

The blink traces were then separated into on and off durations, and weighted probability distributions, $P(\tau_i)$, were obtained by weighting the occurrence of a given on or off duration, $N_{\tau,i}$, by the average time difference from the next longer and shorter durations.

$$P(\tau_i) = \frac{2N_{\tau,i}}{(\tau_{i+1} - \tau_i) + (\tau_i - \tau_{i-1})}$$

For both bin and threshold and CPA methods, fitting of the probability distributions to truncated and nontruncated power laws was carried out in Igor Pro using a nonlinear least-squares fitting procedure.

RESULTS AND DISCUSSION

We studied the blinking kinetics of 17 CdSe/CdS core/shell QDs, of which 8 were 6.8 (0.3) nm in diameter and 9 were 12 (1.3) nm. The probability distributions obtained from binning and thresholding the 17 blink traces are first examined to understand the inherent bias that this method introduces. It is assumed that each blink trace consists of two intensity levels: a low, background-fluorescence level below a threshold referred to as an off state and a high fluorescence, above-threshold on state. It was found that increasing the bin size generally led to a larger measured on-state truncation time τ_c, while increasing the threshold always decreased this truncation time. These findings are in agreement with the theoretical study of Frantsuzov et al.[21] and the experimental results of Crouch et al.[8] and Qin and Guyot-Sionnest.[16] The on-state probability distributions of QD10 obtained for various bin and threshold settings are shown in Figure 1 to illustrate these trends, and the τ_c values for all 17 QDs are summarized in Table S1.

DOI: 10.1021/acs.jpcc.6b09780
J. Phys. Chem. C 2016, 120, 29484−29490

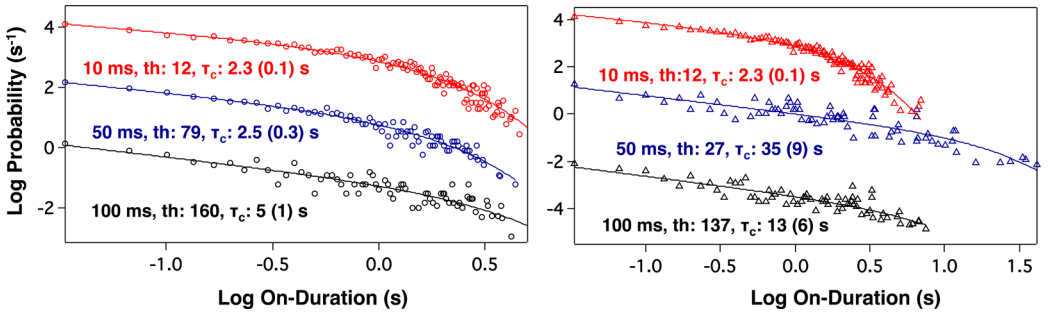

Figure 1. Results of changing bin size and threshold in QD10. Red, blue, and black curves represent on-state probability distributions and corresponding changes in τ_c using 10, 50, and 100 ms bin times, respectively. Circles and triangles represent different threshold locations (noted as "th"). The traces have been vertically offset for clarity.

Next, we turn to the CPA method to analyze blinking in this sample of QDs, where the two-level assumption (employed in the previous method) can be relaxed and the artificial time scale introduced from binning and thresholding removed. As a result, 12 out of 17 QDs had more than two CPA intensity levels (herein, intermediate intensity levels are referred to as gray states) as summarized in Table 1.

Table 1. Number of Intensity Levels in the Measured QDs As Found Using CPA

6.8 nm QDs	no. of levels	12 nm QDs	no. of levels
1	2	9	2
2	2	10	3
3	2	11	3
4	2	12	3
5	3	13	3
6	3	14	3
7	3	15	4
8	4	16	5
		17	5

In comparing the bin and threshold results to those from CPA, we found there is a significant discrepancy in τ_c values. As an example, using the threshold method and a 100 ms bin time, the on-state probability distribution of QD9 cannot be fit to a truncated power law (Figure 2a), while τ_c is 23 (9) and 26 (4) s for 50 and 10 ms bin times, respectively (Figures 2b and 2c, respectively). Expectedly, τ_c is dependent on the choice of bin size. Using the CPA method, QD9 is found to have an on state with an intensity of 2432 cps (counts per second) and a τ_c of 1.7 (0.2) s and a gray state with an intensity of 1748 cps and a τ_c of 3.3 (2) s (Figures 2d and 2e, respectively), where the lowest level is assigned as a gray state due to its high intensity counts. There are two distinct differences between the analysis methods: (a) the truncation times obtained using CPA are different from the bin and threshold values regardless of bin size, and (b) although there are two intensity levels for both methods, the ratio (1.4) between the two CPA intensity levels is too small and the lowest intensity level too high above the background fluorescence for it to be considered an off state.[17] In fact, we find that for 15 QDs the intensity difference between the off and on states is on average 5.0 (1.0) (Table S2). Since 1.4 is significantly smaller than 5.0 (1.0), we can conclude that even though there are two CPA levels, the lowest intensity represents a gray state rather than off state.

In order to understand the origin of this discrepancy, a section of the QD9 blink traces analyzed by both methods is evaluated (Figure 3). To facilitate the comparison of the blink traces and histograms between the two methods, the CPA

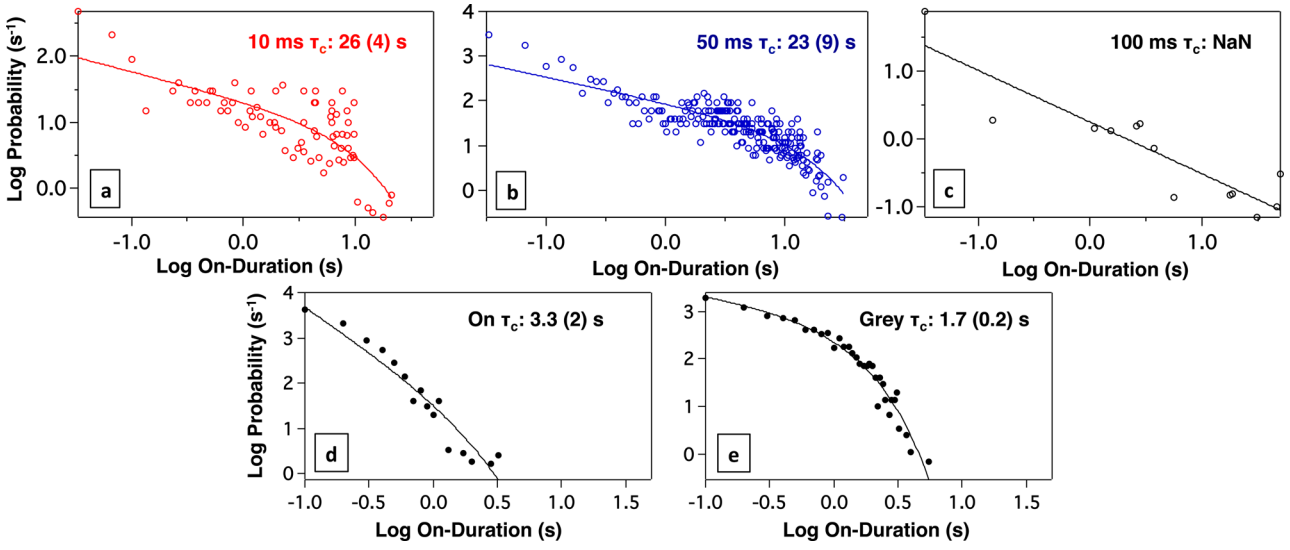

Figure 2. (a), (b), and (c) are the bin and threshold method on-state probability distributions of QD9 for bin sizes 10, 50, and 100 ms, respectively, and (d) and (e) are the CPA probability distributions of two different levels with intensities of 2432 and 1748 cps, respectively.

DOI: 10.1021/acs.jpcc.6b09780
J. Phys. Chem. C 2016, 120, 29484−29490

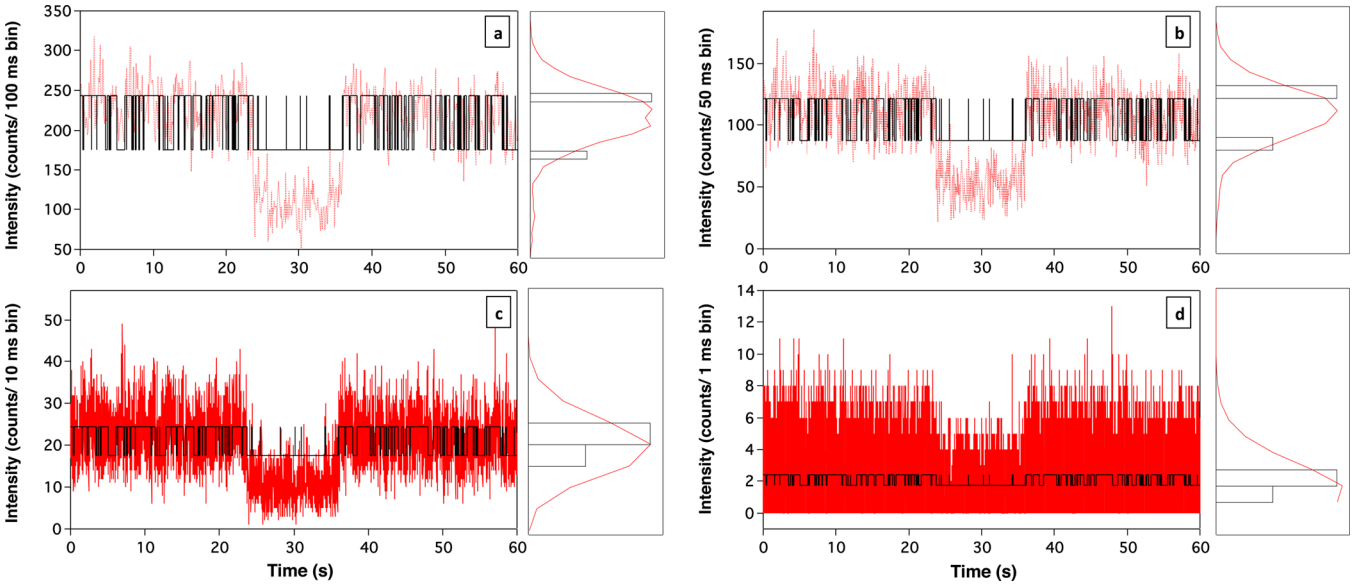

Figure 3. Blink trace of QD9 with bin size (a) 100, (b) 50, (c) 10, and (d) 1 ms, where the red trace is the bin and threshold blink trace and the black is the CPA trace, with the corresponding normalized intensity histograms for both methods. The CPA intensities are multiplied by the bin size used in the bin and threshold method for more facile comparison.

Table 2. τ_c Values of Individual CPA Levels with Corresponding Intensity Counts Compared to the τ_{c_comb} Values from Combined Levels and the Ratio, Δ, Equal to τ_{c_comb}/τ_c[a]

6.8 nm QDs	intensity (cps)	τ_c (s)	τ_{c_comb} (s)	Δ	12 nm QDs	intensity (cps)	τ_c (s)	τ_{c_comb} (s)	Δ
1 on	997	1.1 (0.1)			9 on	1748	3.3 (2)		
2 on	836	3.0 (0.2)			9 gray	2432	1.7 (0.2)		
3 on	1234	0.8 (0.1)			10 on	2684	0.65 (0.06)	1.4 (0.3)	2.2 (0.2)
4 on	1096	2.0 (0.2)			10 gray	1571	1.4 (0.6)		1.0 (0.5)
5 on	2086	1.7 (0.3)	4.7 (0.9)	2.8 (0.3)	11 on	1153	8 (1)	17 (4)	2.1 (0.3)
5 gray	1259	2.2 (0.8)		2.1 (0.4)	12 on	2220	1.4 (0.2)	3.3 (0.4)	2.4 (0.2)
6 on	664	7 (1)	8 (1)	1.1 (0.2)	13 on	3452	0.5 (0.1)	0.62 (0.07)	1.2 (0.2)
7 on	791	10 (2)	16 (5)	1.6 (0.4)	14 on	4330	0.46 (0.08)		
7 gray	414	1.3 (0.4)		12.3 (0.4)	14 gray	3420	0.27 (0.06)		
8 on	1082	1.6 (0.3)	2.0 (0.2)	1.2 (0.2)	14 gray	2169	0.11 (0.02)		
8 gray	797	0.5 (0.2)		4.0 (0.4)	15 on	1961	2.0 (0.2)	7 (1)	3.5 (0.2)
8 gray	450	1.5 (0.6)		1.3 (0.4)	15 gray	1411	0.5 (0.1)		14.0 (0.2)
					15 gray	773	1.61 (0.04)		4.3 (0.1)
					16 on	3525	0.13 (0.02)	10 (2)	76.9 (0.2)
					16 gray	2858	0.30 (0.07)		33.3 (0.3)
					16 gray	1917	0.21 (0.07)		47.6 (0.4)
					17 on	2218	1.3 (0.2)	16 (2)	12.3 (0.2)
					17 gray	1895	0.9 (0.2)		17.8 (0.2)

[a]The CPA intensities are derived using the CPA cluster algorithm.[7]

intensities (in cps) are normalized by multiplying by the bin size (in s) used for the bin and threshold method. In this sample 100 ms-binned blink trace, there is one section from 22 to 35 s where there is a distinct mismatch between CPA and binning and thresholding (Figure 3a). However, as the bin size decreases from 100 to 50 ms (Figure 3b) and then to 10 ms (Figure 3c) and 1 ms (Figure 3d), this discrepancy tends to diminish. This section is most likely a "false off state", arising from averaging photons over a specific bin time and assuming that the lowest intensity is an off state and anything above a set threshold is an on state; i.e., when a threshold is set in QD9, the 22−35 s section will be considered an off state and the rest will be considered on states. In comparison, CPA does not have such a predetermined assumption, and although QD9 has two intensities, the typical two level-assumption (on/off states only) is not invoked and QD9 is found to have one on-state level, one gray state, and no off state.

In contrast to the CPA method, avoiding the two-level assumption when using a bin and threshold analysis proves to be difficult. Decreasing the bin size provides the highest resolution of time scales,[10] but as bin size decreases it becomes more challenging to distinguish levels in intensity histograms. For instance, though the ratio between bright and gray state intensity levels stays the same at 1.4 for the CPA method, it becomes questionable where to set the threshold for bin sizes of 10 and 1 ms (Figures 3c and 3d) in the bin and threshold traces. A similar issue is encountered with increased bin sizes. When the 100 ms intensity histograms of QDs 5, 8, 10, and 15 are compared to those obtained using the CPA method (Figure S3), the bin and threshold histograms appear to have more than

DOI: 10.1021/acs.jpcc.6b09780
J. Phys. Chem. C 2016, 120, 29484−29490

two intensity levels, presumably composed of multiple Gaussian curves with maxima centered near the CPA intensity levels. However, choosing the number of Gaussian curves the histogram should be fit to is ambiguous, and thus both the number and location of intensity levels cannot be reliably obtained using this method. For these reasons, it is often assumed that there are only two intensity levels, where the lowest intensity is considered the off state and anything above is considered an on state.

Because of the aforementioned challenges, we have taken a closer look at QDs that displayed multiple intensity levels using CPA; we explicitly evaluated the two-level assumption in the absence of any preimposed time scale by utilizing the ability to obtain probability distributions for each CPA intensity level. For each multilevel QD, the τ_c values from the probability distributions of individual CPA levels and the τ_{c_comb} values from combining the gray and on-state probability distributions are compared. For instance, QD15 has a total of four levels: an on state, an off state, and two gray states. When the probability distributions are fit for each individual level, the highest three intensity levels of 1961, 1411, and 773 cps have corresponding τ_c values of 2.0 (0.2), 0.5 (0.1), and 1.61 (0.04) s; however, if we assume there is only one on-state level and combine the individual probability distributions, the resulting truncation time (τ_{c_comb}) increases to 7 (1) s. A general trend is apparent that when a two-level assumption is made, the truncation time tends to increase, with the actual magnitude of difference depending on the particular QD. Table 2 summarizes the τ_{c_comb} values from combined levels and the ratio $\Delta = (\tau_{c\_comb}/\tau_c)$, which is always ≥ 1. Figure 4 illustrates this trend, where the

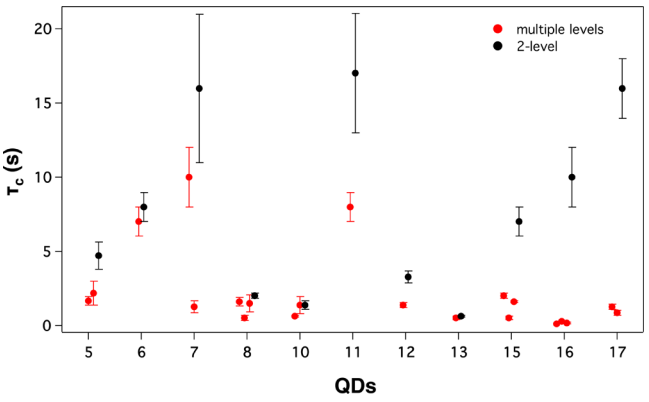

Figure 4. Red circles represent the τ_c values of individual levels, and black circles are the τ_{c_comb} values from combined levels. The error bars represent the standard deviation.

black circles representing the τ_{c_comb} are consistently larger than the red circles representing the τ_c values of the individual levels. It should be noted that it is reasonable to observe a longer τ_c when intensity levels are combined. As an example, within a 5 s window containing two levels, one level may be 3 s in duration and the other level 2 s; when these are combined into one level with a 5 s duration, the probability distribution will contain longer on-state durations and therefore a longer truncation time.

Assuming that the bias arising from binning and thresholding blink traces is largely eliminated with CPA, there still exists uncertainty as to whether these multiple levels have real physical origins, meaning they arise from different emissive states. In order to evaluate such an issue, both the validity of the CPA method with respect to detecting multiple levels and the physical origin of these levels must be understood.

CPA uses an algorithm called Bayesian information criteria (BIC) (also known as Schwartz's criterion)[7]

$$\mathrm{BIC} = 2\mathcal{L}_G - (2n_G - 1)\ln N_{cp} - N_{cp}\ln N$$

to determine the number of levels, where N_{cp} is the number of change points, N is the total number of photons, and $\mathcal{L}_G$ is the log-likelihood, evaluating how accurately the n_G or the number of states represents the original data. The n_G that gives the maximum BIC value represents the most likely number of levels that are contained in the trajectory. The performance of BIC increases with the number of change points detected; for instance, with 500 change points detected, the accuracy of CPA exceeds 90%. However, the absolute value of the uncertainty increases as the number of levels increases. As an illustration of the effect of N_{cp} and number of levels on the accuracy (or uncertainty), for trajectories with two levels the absolute uncertainty is less than 3% when the N_{cp} is 50, and for those with six levels the uncertainty is less than 5% when N_{cp} is 500. The uncertainty is always less than 5% for the data reported considering the N_{cp} detected in the 17 QDs (Table S3).

Despite this ability to quantify the absolute uncertainty, there exists ambiguity in detecting all the change points due to the choice of the correct parameters for the acceptable level of false positives in hypothesis tests, as stated in the work of Houel et al.[9] and Watkins and Yang.[7] False positives refer to the detection of change points that do not correspond to real states. An allowed value of false positives must be selected to maximum the efficiency of detecting all change points while minimizing the detection of false change points.[9] In order to address this issue, different values of allowed false positives are input into the CPA analysis, and the reconstructed CPA blink traces are cross-correlated to those obtained from a minimum binning approach. This process is explained in detail in the Supporting Information. Briefly, the minimum bin approach, where there is at least one photon in each bin, is selected as it gives the highest time resolution and widest range of time scales, comparable to CPA.[10] The two blink traces are cross-correlated with a zero time delay, and a cross-correlation coefficient is calculated. The highest cross-correlation coefficient represents the closest match between the CPA blink trace and minimal binning approach. In this study, we found that the values 0.01 and 0.95 for detecting false change points and the confidence interval, respectively, gave the largest cross-correlation coefficient (Table S3). These values can be interpreted as a 1% probability of detecting false change points among a number of N detected change points and a 95% confidence that the true change point lies in the calculated confidence region. Different scenarios of these values for various systems of number of photons detected and intensity ratios between levels have been previously demonstrated.[7]

Having addressed the accuracy of the CPA method in detecting multiple levels, possible explanations for the physical origins of multiple intensity levels can be reviewed. Gray state emission has been observed in several studies, although the conclusions on what gives rise to an intermediate emissive level have varied.[4,16−19,22−25] Two early studies attributed the appearance of a gray state in CdSe/CdS QDs to positive trions created via electron ionization[17] or electron surface trapping,[19] on the basis of the electron being delocalized across the QD core and shell while the hole remains localized in the

DOI: 10.1021/acs.jpcc.6b09780
J. Phys. Chem. C 2016, 120, 29484−29490

core. Conversely in the same material, Qin and Guyot-Sionnest assigned the gray state to negative trions formed from hole trapping to shallow surface states, based on the similarity between the negative trion lifetime and the gray state lifetime.[16] A later experiment measured blinking in CdSe/CdS seeded rods with PbS tips that result in an engineered deep hole trap; upon introduction of the deep hole trap, the appearance of gray state emission at the expense of the on state was attributed to negative trions.[18]

There are additional models that propose origins for gray states that are not due to trions. For example, a charge-tunneling and self-trapping (CTST) model recently proposed by Osborne and Fisher provides an origin for the gray state that is shell thickness dependent.[25] In the CTST model framework, the bright and gray states in thin-shelled QDs arise from surface-charged ionized exciton states and mixed contributions including the neutral, emissive core-exciton state, respectively. With increasing shell thickness, the modulation depth between the surface-charged states and the neutral emissive state increases as the surface-charged exciton states become quenched relative to the latter. As a result, the gray and bright intensity levels become further separated and are more easily resolved with increasing shell thickness. This finding is consistent with the results presented here: all of the nine 12 nm QDs exhibited resolvable gray state emission while only four out of eight of the 6.8 nm QDs did the same.

The multiple recombination center (MRC) model attributes blinking to a fluctuating nonradiative rate. Specifically, fluctuations are proposed to occur in the hole trapping rate via surface quenching centers that can switch between active (high hole trapping rate) and inactive (low hole trapping rate) conformations; hole trapping to the recombination centers (RC) is then followed by nonradiative recombination.[21] The MRC model can naturally predict a continuous distribution of intensities, and an observation of increased gray states in thicker shelled QDs could be expected. As the shell thickness is increased, surface RCs are placed further away from the localized hole in the QD core, which leads to a decrease in the trapping strength of RCs in the active conformation. The MRC model has been able to account for high, medium, and low intensity levels in CdSe/CdS QDs through the combination of one weak RC and a few strong RCs.[4] It is reasonable to expect a higher number of these weak RCs relative to strong ones as shell thickness is increased, and thus one would expect, within the MRC model framework, to observe more gray states in thicker shelled QDs. The average number of emission states for the 12 (1.3) nm QDs, 3.4, is indeed larger than that of the 6.8 (0.3) nm QDs, 2.6.

While the MRC result was obtained using a power spectral density analysis, the previous referenced works relied on the bin and threshold method. Gray state emission was observed in binned intensity histograms with small bin sizes (<10 ms), with the gray state peak vanishing when the binning time is increased. However, even if gray states can be detected in intensity histograms using small bin sizes, investigating their kinetics remains very challenging since the gray state kinetics may be unresolved from the on- or off-state kinetics depending on the choice of bin and threshold. In addition, as was pointed out previously, a statistically rigorous assignment of the number and location of emissive states using the bin and threshold method is ambiguous. While in previous experiments that analyze gray states via the bin and threshold method, the gray state probability distribution was found to follow exponential or stretched exponential kinetics,[16,18,19] in this CPA study, gray states were observed to exhibit power-law kinetics similar to the on and off states. As an accurate description on the origins of gray states relies largely on the ability to fit probability distributions while avoiding biases associated with binning and thresholding, the CPA method offers a reliable and robust means to detecting and elucidating the kinetics of gray state emission in single QDs.

CONCLUSION

In this study, we have used change point analysis to study the biases associated with analyzing the kinetics of quantum dot blinking. It is a commonly used assumption that there is one on and one off state when using the bin and threshold method. Using CPA, we have identified that in most QDs studied here, there are more than just one on and one off state, prompting us to re-evaluate the two-level assumption. We found that the truncation time (τ_c) from the probability distributions of individual levels is significantly different compared to the τ_c obtained using the two-level assumption. The performance and validity of the CPA method are evaluated, and the physical origins of gray state emission are discussed. In the QDs investigated in this work, we found that the two-level assumption was not valid, and multilevel emission could be more accurately studied using the CPA method in place of the more traditional bin and threshold method.

ASSOCIATED CONTENT

Supporting Information

The Supporting Information is available free of charge on the ACS Publications website at DOI: 10.1021/acs.jpcc.6b09780.

Change point analysis and hypothesis test values, photon-correlation antibunching trace, intensity level histograms, alpha and beta values, and table of on- and off-state truncation times using the bin and threshold method (PDF)

AUTHOR INFORMATION

Corresponding Author

*E-mail srl@berkeley.edu; Fax +1 510-643-1376; Tel +1 510-643-5467 (S.R.L.).

ORCID

A. Paul Alivisatos: 0000-0001-6895-9048

Present Address

Y.J.B.: Department of Chemistry, Northwestern University, Evanston, IL 60208.

Author Contributions

Y.J.B. and N.A.G. contributed equally to this work.

Notes

The authors declare no competing financial interest.

ACKNOWLEDGMENTS

This work was supported by the U.S. Department of Energy, Office of Science, Basic Energy Sciences, Materials Sciences and Engineering Division under Award # DE-AC02-05CH11231 within the PChem program (KC3103). Y.B. acknowledges support provided by the National Science Foundation under Grant NSF-CHE-1361226, the Air Force Office of Scientific Research (AFOSR-FA9550-14-1-0154), and ARO-MURI#1-W911NF-14-1-0383. T.X.D. acknowledges the National

DOI: 10.1021/acs.jpcc.6b09780
J. Phys. Chem. C 2016, 120, 29484−29490

Science Foundation Graduate Research Fellowship under Grant DGE 1106400.

REFERENCES

(1) Cordones, A. A.; Leone, S. R. Mechanisms for Charge Trapping in Single Semiconductor Nanocrystals Probed by Fluorescence Blinking. *Chem. Soc. Rev.* **2013**, *42*, 3209−3221.
(2) Shimizu, K.; Neuhauser, R.; Leatherdale, C.; Empedocles, S.; Woo, W.; Bawendi, M. Blinking Statistics in Single Semiconductor Nanocrystal Quantum Dots. *Phys. Rev. B: Condens. Matter Mater. Phys.* **2001**, *63*, 205316/1−205316/5.
(3) Galland, C.; Ghosh, Y.; Steinbrück, A.; Sykora, M.; Hollingsworth, J. A.; Klimov, V. I.; Htoon, H. Two Types of Luminescence Blinking Revealed by Spectroelectrochemistry of Single Quantum Dots. *Nature* **2011**, *479*, 203−207.
(4) Frantsuzov, P.; Kuno, M.; Jankó, B.; Marcus, R. A. Universal Emission Intermittency in Quantum Dots, Nanorods and Nanowires. *Nat. Phys.* **2008**, *4*, 519−522.
(5) Chung, I.; Bawendi, M. G. Relationship between Single Quantum-Dot Intermittency and Fluorescence Intensity Decays from Collections of Dots. *Phys. Rev. B: Condens. Matter Mater. Phys.* **2004**, *70*, 165304/1−165304/5.
(6) Peterson, J. J.; Nesbitt, D. J. Modified Power Law Behavior in Quantum Dot Blinking: A Novel Role for Biexcitons and Auger Ionization. *Nano Lett.* **2009**, *9*, 338−345.
(7) Watkins, L. P.; Yang, H. Detection of Intensity Change Points in Time-Resolved Single-Molecule Measurements. *J. Phys. Chem. B* **2005**, *109*, 617−628.
(8) Crouch, C. H.; Sauter, O.; Wu, X.; Purcell, R.; Querner, C.; Drndic, M.; Pelton, M. Facts and Artifacts in the Blinking Statistics of Semiconductor Nanocrystals. *Nano Lett.* **2010**, *10*, 1692−1698.
(9) Houel, J.; Doan, Q. T.; Cajgfinger, T.; Ledoux, G.; Amans, D.; Aubret, A.; Dominjon, A.; Ferriol, S.; Barbier, R.; Nasilowski, M.; et al. Autocorrelation Analysis for the Unbiased Determination of Power-Law Exponents in Single-Quantum-Dot Blinking. *ACS Nano* **2015**, *9*, 886−893.
(10) Yang, H.; Xie, X. S. Probing Single-Molecule Dynamics Photon by Photon. *J. Chem. Phys.* **2002**, *117*, 10965−10979.
(11) Volkán-Kacsó, S. Two-State Theory of Binned Photon Statistics for a Large Class of Waiting Time Distributions and its Application to Quantum Dot Blinking. *J. Chem. Phys.* **2014**, *140*, 224110/1−224110/13.
(12) Gopich, I. V.; Szabo, A. Theory of the Statistics of Kinetic Transitions with Application to Single-Molecule Enzyme Catalysis. *J. Chem. Phys.* **2006**, *124*, 154712/1−154712/21.
(13) Pelton, M.; Grier, D. G.; Guyot-Sionnest, P. Characterizing Quantum-Dot Blinking Using Noise Power Spectra. *Appl. Phys. Lett.* **2004**, *85*, 819−821.
(14) Pelton, M.; Smith, G.; Scherer, N. F.; Marcus, R. A. Evidence for a Diffusion-Controlled Mechanism for Fluorescence Blinking of Colloidal Quantum Dots. *Proc. Natl. Acad. Sci. U. S. A.* **2007**, *104*, 14249−14254.
(15) Messin, G.; Hermier, J. P.; Giacobino, E.; Desbiolles, P.; Dahan, M. Bunching and Antibunching in the Fluorescence of Semiconductor Nanocrystals. *Opt. Lett.* **2001**, *26*, 1891−1893.
(16) Qin, W.; Guyot-Sionnest, P. Evidence for the Role of Holes in Blinking: Negative and Oxidized CdSe/CdS Dots. *ACS Nano* **2012**, *6*, 9125−9132.
(17) Spinicelli, P.; Buil, S.; Quélin, X.; Mahler, B.; Dubertret, B.; Hermier, J. P. Bright and Grey States in CdSe-CdS Nanocrystals Exhibiting Strongly Reduced Blinking. *Phys. Rev. Lett.* **2009**, *102*, 136801/1−136801/4.
(18) Tenne, R.; Teitelboim, A.; Rukenstein, P.; Dyshel, M.; Mokari, T.; Oron, D.; Systems, C.; Sheva, B.; Tenne, R.; Teitelboim, A.; et al. Studying Quantum Dot Blinking through the Addition of an Engineered Inorganic Hole Trap. *ACS Nano* **2013**, *7*, 5084−5090.
(19) Gómez, D. E.; Van Embden, J.; Mulvaney, P.; Fernée, M. J.; Rubinsztein-Dunlop, H. Exciton-Trion Transitions in Single CdSe-CdS Core-Shell Nanocrystals. *ACS Nano* **2009**, *3*, 2281−2287.
(20) Chen, O.; Zhao, J.; Chauhan, V. P.; Cui, J.; Wong, C.; Harris, D. K.; Wei, H.; Han, H.-S.; Fukumura, D.; Jain, R. K. Compact High-Quality CdSe-CdS Core-Shell Nanocrystals with Narrow Emission Linewidths and Suppressed Blinking. *Nat. Mater.* **2013**, *12*, 445−451.
(21) Frantsuzov, P. A.; Volkán-Kacsó, S.; Jankó, B. Model of Fluorescence Intermittency of Single Colloidal Semiconductor Quantum Dots Using Multiple Recombination Centers. *Phys. Rev. Lett.* **2009**, *103*, 207402/1−207402/4.
(22) Verberk, R.; van Oijen, A.; Orrit, M. Simple Model for the Power-Law Blinking of Single Semiconductor Nanocrystals. *Phys. Rev. B: Condens. Matter Mater. Phys.* **2002**, *66*, 233202/1−233202/4.
(23) Fisher, B.; Eisler, H.; Stott, N. E.; Bawendi, M. G. Emission Intensity Dependence and Single-Exponential Behavior in Single Colloidal Quantum Dot Fluorescence Lifetimes. *J. Phys. Chem. B* **2004**, *108*, 143−148.
(24) Zhang, K.; Chang, H.; Fu, A.; Alivisatos, A. P.; Yang, H. Continuous Distribution of Emission States from Single CdSe/ZnS Quantum Dots. *Nano Lett.* **2006**, *6*, 843−847.
(25) Osborne, M. A.; Fisher, A. A. E. Charge-Tunnelling and Self-Trapping: Common Origins for Blinking, Grey-State Emission and Photoluminescence Enhancement in Semiconductor Quantum Dots. *Nanoscale* **2016**, *8*, 9272−9283.

DOI: 10.1021/acs.jpcc.6b09780
J. Phys. Chem. C 2016, 120, 29484−29490